



AFRL-RX-WP-TP-2009-4087

RELAXATION BEHAVIOR OF Ca-BASED BULK METALLIC GLASSES (PREPRINT)

Oleg N. Senkov and Daniel B. Miracle

UES, Inc.

APRIL 2009

Approved for public release; distribution unlimited.

See additional restrictions described on inside pages

STINFO COPY

**AIR FORCE RESEARCH LABORATORY
MATERIALS AND MANUFACTURING DIRECTORATE
WRIGHT-PATTERSON AIR FORCE BASE, OH 45433-7750
AIR FORCE MATERIEL COMMAND
UNITED STATES AIR FORCE**

REPORT DOCUMENTATION PAGE

*Form Approved
OMB No. 0704-0188*

The public reporting burden for this collection of information is estimated to average 1 hour per response, including the time for reviewing instructions, searching existing data sources, searching existing data sources, gathering and maintaining the data needed, and completing and reviewing the collection of information. Send comments regarding this burden estimate or any other aspect of this collection of information, including suggestions for reducing this burden, to Department of Defense, Washington Headquarters Services, Directorate for Information Operations and Reports (0704-0188), 1215 Jefferson Davis Highway, Suite 1204, Arlington, VA 22202-4302. Respondents should be aware that notwithstanding any other provision of law, no person shall be subject to any penalty for failing to comply with a collection of information if it does not display a currently valid OMB control number. **PLEASE DO NOT RETURN YOUR FORM TO THE ABOVE ADDRESS.**

1. REPORT DATE (DD-MM-YY) April 2009			2. REPORT TYPE Journal Article Preprint		3. DATES COVERED (From - To) 01 April 2009- 01 April 2009	
4. TITLE AND SUBTITLE RELAXATION BEHAVIOR OF Ca-BASED BULK METALLIC GLASSES (PREPRINT)			5a. CONTRACT NUMBER FA8650-04-D-5235			
			5b. GRANT NUMBER			
			5c. PROGRAM ELEMENT NUMBER 62102F			
6. AUTHOR(S) Oleg N. Senkov (UES, Inc.) Daniel B. Miracle (AFRL/RXLMD)			5d. PROJECT NUMBER 2511			
			5e. TASK NUMBER 00			
			5f. WORK UNIT NUMBER 25110002			
7. PERFORMING ORGANIZATION NAME(S) AND ADDRESS(ES) UES, Inc. 4401 Dayton, Xenia Road Dayton, OH 45433-7817			Metals Branch (RXLMD) Metals, Ceramics and NDE Division Materials and Manufacturing Directorate Wright-Patterson Air Force Base, OH 45433-7750 Air Force Materiel Command, United States Air Force		8. PERFORMING ORGANIZATION REPORT NUMBER AFRL-RX-WP-TP-2009-4087	
9. SPONSORING/MONITORING AGENCY NAME(S) AND ADDRESS(ES) Air Force Research Laboratory Materials and Manufacturing Directorate Wright-Patterson Air Force Base, OH 45433-7750 Air Force Materiel Command United States Air Force			10. SPONSORING/MONITORING AGENCY ACRONYM(S) AFRL/RXLMD		11. SPONSORING/MONITORING AGENCY REPORT NUMBER(S) AFRL-RX-WP-TP-2009-4087	
12. DISTRIBUTION/AVAILABILITY STATEMENT Approved for public release; distribution unlimited.						
13. SUPPLEMENTARY NOTES To be submitted to Metallurgical and Materials Transactions A PAO Case Number and clearance date: 88ABW-2009-1275, 01 April 2009. The U.S. Government is joint author of this work and has the right to use, modify, reproduce, release, perform, display, or disclose the work.						
14. ABSTRACT Relaxation behavior of Ca60Mg20Zn20, Ca60Mg20Cu20, Ca65Mg15Zn20, Ca50Mg20Cu30, and Ca55Mg18Zn11Cu16 bulk metallic glasses was determined in the glass transition region using DSC with the heating rates from 1 to 160 K/min. The activation enthalpy of structural relaxation and the fragility index m were found to be smaller in the glassy state (onset of the glass transition) than in the supercooled liquid state (end of glass transition). The Ca-based glass-forming liquids showed strong behavior of the relaxation time, with the fragility indexes m in the range of 33 to 40. The strong liquid behavior implies sluggish kinetics of crystallization in the supercooled liquid region and explain the very good glass forming ability of these alloys. The critical cooling rate for amorphization R_c of the Ca-based bulk metallic glasses was estimated to be in the range of 0.3 to 10 K/s, which is similar to R_c values for the best Pd and Zr based metallic glass forming alloys discovered so far.						
15. SUBJECT TERMS bulk metallic glasses, Ca-based						
16. SECURITY CLASSIFICATION OF: a. REPORT Unclassified		17. LIMITATION OF ABSTRACT: b. ABSTRACT Unclassified	18. NUMBER OF PAGES c. THIS PAGE Unclassified	19a. NAME OF RESPONSIBLE PERSON (Monitor) Jonathan E. Spowart 19b. TELEPHONE NUMBER (Include Area Code) N/A		

Relaxation Behavior of Ca-based Bulk Metallic Glasses

Oleg N. Senkov¹ and Daniel B. Miracle

Air Force Research Laboratory, Materials and Manufacturing Directorate, Wright-Patterson AFB, OH 45433.

ABSTRACT

Relaxation behavior of $\text{Ca}_{60}\text{Mg}_{20}\text{Zn}_{20}$, $\text{Ca}_{60}\text{Mg}_{20}\text{Cu}_{20}$, $\text{Ca}_{65}\text{Mg}_{15}\text{Zn}_{20}$, $\text{Ca}_{50}\text{Mg}_{20}\text{Cu}_{30}$, and $\text{Ca}_{55}\text{Mg}_{18}\text{Zn}_{11}\text{Cu}_{16}$ bulk metallic glasses was determined in the glass transition region using differential scanning calorimetry (DSC) with the heating rates from 1 to 160 K/min. The activation enthalpy of structural relaxation and the fragility index m were found to be smaller in the glassy state (onset of the glass transition) than in the supercooled liquid state (end of glass transition). The Ca-based glass-forming liquids showed strong behavior of the relaxation time, with the fragility indexes m in the range of 33 to 40. The strong liquid behavior implies sluggish kinetics of crystallization in the supercooled liquid region and explains the very good glass forming ability of these alloys. The critical cooling rate for amorphization R_c of the Ca-based bulk metallic glasses was estimated to be in the range of 0.3 to 10 K/s, which is similar to R_c values for the best Pd and Zr based metallic glass forming alloys discovered so far.

INTRODUCTION

Depending on the temperature dependence of the relaxation time τ (or equivalently, the viscosity $\eta = G_\infty \tau$, where G_∞ is the dynamic shear modulus) in the temperature range between T_g and T_m , where T_g is the glass transition temperature and T_m is the melting (usually liquidus) temperature,

¹ Corresponding author. Mailing address is UES, Inc., 4401 Dayton-Xenia Rd., Dayton, OH 45432-1892, USA; Phone: 937-255-1320; e-mail: oleg.senkov@wpafb.af.mil.

glass forming liquids are divided into strong and fragile liquids. When the logarithm of the relaxation time of a supercooled liquid is plotted versus an inverse absolute temperature, T , reduced by T_g (i.e. $\log(\tau)$ vs. T_g/T), all glass forming liquids have the same relaxation time of $\tau_g = 10^3$ s at $T = T_g$ (in accord to this definition of T_g) [1]. With an increase in temperature above T_g , liquids with strong directional bonding and high stability of intermediate range order, such as silica or germania, show almost a linear, Arrhenius, dependence of $\log(\tau)$ on T_g/T over the whole temperature range above T_g . These liquids are called *strong liquids*. At the same time, molecular liquids and many metallic glasses, which lack a strong directional bonding character and therefore possess a high configurational degeneracy and suffer rapid degradation of intermediate range order above T_g , show a very rapid decrease in $\log(\tau)$ with a decrease in T_g/T in the temperature range of $T_g \leq T \leq T_m$, and a weak dependence above T_m . These liquids are called *fragile liquids*. Examples of extremely fragile liquids are o-terphenyl, toluene, pure metals and marginal metallic glasses. Stronger liquids are generally better glass formers because they have higher viscosity /relaxation time at $T < T_m$ and, therefore, slower kinetics of crystallization, than more fragile liquids [2,3,4]. Almost all bulk metallic glasses show intermediate fragile behavior [5]. Slow kinetics of crystallization due to high viscosity / high relaxation time of supercooled liquid can also be important for enhancing GFA of bulk metallic glasses

The fragile behavior of supercooled glass forming liquids can generally be described by an empirical Vogel-Fulcher -Tamman (VFT) equation [6]:

$$\tau = \tau_\infty \exp[A/(T-T_o)] \quad (1)$$

where τ_∞ , A and T_o are fitting parameters. An approach to quantify liquid fragility defines a fragility index m as the slope of the $\log_{10}\tau$ (or $\log_{10}\eta$) vs T_g/T curve near T_g [7]:

$$m = \frac{d \log_{10} \tau}{d(T_g/T)} \Big|_{T=T_g} \equiv \frac{d \log_{10} \eta}{d(T_g/T)} \Big|_{T=T_g} \quad (2)$$

According to this definition, more fragile liquids have higher m values.

Since its introduction in 1993, the fragility index m has become an important material constant, which has been found to correlate with other glass properties, such as vibrational properties of the harmonic glassy dynamics [8], Poisson's ratio [9,10], jump in the heat capacity at T_g [11,12] and GFA [4,13]. For example, the critical cooling rate for amorphization, R_c , was found to increase with an increase in the fragility index m , obeying the following relation [4]:

$$\log(R_c) = 11.8 - 694/[32+m(1/T_{rg}-1)] \quad (3)$$

where R_c is given in K/s and $T_{rg} = T_g/T_m$ is the reduced glass transition temperature.

Although m describes the viscous behavior of a super-cooled liquid near T_g , recent analysis [14] has shown that, together with other experimentally accessible parameters, it can be used to describe the temperature dependence of viscosity in a wider temperature range:

$$\log(\eta) = 12 - n \frac{1 - \frac{T_g}{T}}{1 - \left(1 - \frac{n}{m}\right) \frac{T_g}{T}} \quad (4)$$

In equation (4), $n = m \frac{1 - (1 - T_{rg}) \frac{\Delta C_p(T_g)}{\Delta S_m}}{1 + T_{rg} \frac{\Delta C_p(T_g)}{\Delta S_m}}$, $\Delta C_p(T_g)$ is the heat capacity jump at T_g and $\Delta S(T_m)$ is the entropy of fusion.

The above brief overview clearly indicates a significant importance of the fragility index m for linking dynamic and thermodynamic properties of supercooled liquid and glassy states. From this perspective, it is critical to establish experimental procedures for measuring correct values of

m for different glass forming liquids. Two main methods to measure m are widely used. The first is the straightforward method of measuring the steepness of the $\log \eta$ vs T_g/T and/or $\log \tau$ vs T_g/T curves at T_g , in accord to Equation (2), using reliable viscosity or relaxation time data for the supercooled liquid state in the temperature range close to T_g . An extensive m database compiled by this direct method is currently available for many oxide and organic liquids [7,11,15], as well as for some metallic alloys [10,16]. The fragility index obtained by this method is called *kinetic fragility index* and is identified as m_k .

The second method involves differential scanning calorimetry (DSC) at a constant heating (or cooling) rate φ . This approach uses the fact that, upon heating, the glass transition represents the relaxation of the non-equilibrium glassy state into the equilibrium supercooled liquid state. Kinetics of the glass transition reflects the relationship between the relaxation time and temperature. When a higher heating rate φ is used, the calorimetric glass transition temperature T_g^{cal} shifts to a higher temperature. This dependence of T_g^{cal} on φ is used to calculate the activation enthalpy of structural relaxation, ΔH_g , at the glass transition [17]:

$$\Delta H_g = -R \frac{d \ln \varphi}{d(1/T_g^{cal})} \quad (5)$$

where R is the gas constant. The *calorimetric fragility index* m_c is then often calculated as:

$$m_c = \frac{\Delta H_g}{RT_g^{ref} \ln 10} \quad (6)$$

In equation (6), T_g^{ref} is the calorimetric glass transition temperature determined at a referenced heating rate φ^{ref} . The latter can be defined as $\varphi^{ref} = \Delta T_g / \tau_g$, where $\Delta T_g = T_{ge} - T_{gs}$ is the temperature interval of the glass transition, T_{gs} and T_{ge} are the temperatures of the start and the end of the glass transition, respectively, and $\tau_g = 1000$ s. Equation (6) is equivalent to Equation

(2) only if ΔT_g is essentially independent of the heating rate, which is not always correct [1,18].

In general, use of the total relaxation time for the calorimetric glass transition, $\tau_g^{cal} = \Delta T_g / \varphi$,

instead of φ , is more appropriate [19,20], and m_c is calculated as the slope of $\log \tau_g^{cal}$ vs. $1/T_g^{cal}$

reduced by T_g^{ref} :

$$m_c = \frac{1}{T_g^{ref}} \frac{\Delta \log \tau_g^{cal}}{\Delta(1/T_g^{cal})} \Big|_{T_g^{ref}} \quad (7)$$

The m_c -values obtained by DSC are almost always smaller than m_k -values obtained from viscosity / relaxation time measurements [10,15,17]. For example, $m_k = 50, 59$, and 54 vs. $m_c = 39, 52$, and 41 were reported for $Zr_{41}Ti_{14}Cu_{12.5}Ni_{10}Be_{22.5}$, $Pd_{39}Ni_{10}Cu_{30}P_{21}$, and $Pd_{40}Ni_{40}P_{20}$, respectively [10]. In our opinion, the reason of such discrepancy is using the temperature of the onset of the glass transition, i.e. T_{gs} , as T_g^{cal} in equations (6) and (7). Indeed, analysis of all experimental data on calorimetric measurements of m_c for bulk metallic glasses reported to date shows that only the time dependence of T_{gs} has been used. However, T_{gs} corresponds to the glassy state and, therefore, m_c determined in this way reflects the relaxation behavior of the glassy state, while m_k , by definition, reflects the relaxation behavior of a supercooled liquid state at T_g . We therefore suggest here that, in order to correctly determine the relaxation behavior of a supercooled liquid near T_g in DSC experiments, the temperature of the end of the glass transition, i.e. T_{ge} , should be used as T_g^{cal} in Equations (6) and/or (7), because, within the glass transition range, this temperature most closely corresponds to the supercooled liquid state.

In this paper, we report on the relaxation behavior of several Ca-Mg-Zn, Ca-Mg-Cu and Ca-Mg-Zn-Cu bulk metallic glasses (BMGs) determined by DSC in the glass transition range. These relatively new amorphous metallic materials are based on two simple metals, Ca and Mg, have

the lowest density among all BMGs discovered so far, and have excellent glass forming ability (GFA) [21,22,23,24,25,26,27]. The relaxation behavior of these materials in the glassy state, using T_{gs} as T_g^{cal} , is shown to be stronger than in the supercooled liquid state, where T_g^{cal} is given by T_{ge} . The fragile behavior of the Ca-based BMGs is compared with the behavior of other metallic and non-metallic glasses / supercooled liquids. It is concluded that the Ca-based supercooled liquids are less fragile than other BMGs, and their fragility is comparable with the fragility of strong oxide glasses. The GFA of the Ca-based BMGs is estimated to be similar to GFA of best glass-forming Pd-based and Zr-based BMGs.

EXPERIMENTAL PROCEDURES

Five Ca-based glassy alloys were prepared by a Cu-mold casting method in the form of 4-mm thick plates. The nominal alloy compositions, in atomic %, are Ca₆₀Mg₂₀Zn₂₀, Ca₆₀Mg₂₀Cu₂₀, Ca₆₅Mg₁₅Zn₂₀, Ca₅₀Mg₂₀Cu₃₀, and Ca₅₅Mg₁₈Zn₁₁Cu₁₆. The methods of the alloy preparation and casting, as well as some thermodynamic properties of these glassy alloys, were reported elsewhere [21,23,24]. The DSC heating runs of the amorphous samples were conducted on a TA Instruments Q-1000 differential scanning calorimeter in the temperature range of 330K to 450K, which covered the glass transition region, with heating rates of 1.0, 2.5, 5.0, 10, 20, 40, 80, 110 and 160 K/min. The temperatures T_{gs} and T_{ge} , as well as ΔT_g , were determined at different heating rates using TA Universal Analysis version 4.2E software. From the rate dependences of T_{gs} and T_{ge} , the activation enthalpy of the structural relaxation ΔH_g and the fragility index m_c were determined in the glassy and supercooled liquid regions near the glass transition with the use of Equations (5) and (7), respectively.

RESULTS

Figure 1 illustrates a typical DSC scan at the heating rate of 20 K/min of the Ca₅₀Mg₂₀Cu₃₀ BMG. The glass, glass transition and supercooled liquid temperature regions are clearly identified. The glass transition starts at T_{gs} and ends at T_{ge} , while the supercooled liquid region is terminated by crystallization at T_x . More examples of DSC scans for the Ca-based BMGs can be found in previous publications [21,23,24,28].

The dependences of T_{gs} and T_{ge} on heating rate for two Ca-based BMGs are shown in Figure 2. Both T_{gs} and T_{ge} increase and the temperature interval of the glass transition ΔT_g decreases with an increase in the heating rate. From the dependences of T_{gs} and T_{ge} on the heating rate, the activation enthalpies of structural relaxation at the beginning (ΔH_{gs}) and the end (ΔH_{ge}) of glass transition were calculated using Equation (5) and their values are given in Table 1. The m_c values calculated with Equation (6) are also given in this table. It can be seen that the ternary Ca-based BMGs have almost the same $\Delta H_{gs} \approx 121\text{-}127$ kJ/mol, while the quaternary Ca₅₅Mg₁₈Zn₁₁Cu₁₆ alloy has slightly higher $\Delta H_{gs} = 134$ kJ/mol. The relaxation enthalpy increases with an increase in the volume fraction of the supercooled liquid, and at the end of the glass transition $\Delta H_{ge} = 211\text{-}229$ kJ/mol for the ternary alloys and 255 kJ/mol for the quaternary alloy.

Figure 3 shows the dependences of the total relaxation time for the glass transition,

$\tau_g^{cal} = \Delta T_g / \varphi$, on T_{gs} and T_{ge} plotted in Arrhenius coordinates, i.e. $\log \tau_g^{cal}$ vs. $1/T$. These dependences were fitted with the VFT Equation (1), in which $\tau_\infty = 10^{-14}$ s was assigned based on earlier observations [6,7] that (i) for many glass forming liquids τ_∞ is in the range of $10^{-15.5} - 10^{-12.5}$ s and (ii) the VFT fit of the temperature dependence of the relaxation time near T_g is not very sensitive to the exact value of τ_∞ in the given τ_∞ range. The VFT fitting parameters A and T_o (Equation 1) for five Ca-based BMGs studied in this work are given in Tables 2 and 3 for the

onset and the end of the glass transition, respectively. Using these fitting parameters, the reference glass transition temperatures T_{gs}^{ref} and T_{ge}^{ref} for the onset and the end of the glass transition, respectively, were determined, using Equation (1), as the temperatures at which $\tau_g^{cal} = 1000$ s, i.e.

$$T_g^{ref} = T_o + A/(17\ln 10) \approx T_o + 0.0255A \quad (8)$$

Finally, the fragility index m_c was calculated for the onset and the end of the glass transition using Equation (7) and the VFT fitting curves (Equation 1) [7]:

$$m_c = \frac{AT_g^{ref}}{(T_g^{ref} - T_o)^2 \ln 10} \quad (9)$$

The calculated T_g^{ref} and m_c values for the Ca-based BMGs at the onset and the end of the glass transition are tabulated in Tables 2 and 3, respectively.

DISCUSSION

The results reported in this work clearly indicate that the relaxation behavior of Ca-based BMGs in the glass transition region is different at the onset and the end of the glass transition. The enthalpy of the structural relaxation ΔH_g and the fragility index m_c were found to be smaller at the onset than at the end of the glass transition (see Tables 1-3). The parameters of the VFT Equation (1) are also different so that A is higher and T_o is smaller for relaxation at the onset than at the end of the glass transition (compare Tables 2 and 3). Taking into account that the liquid fragility increases with an increase in m and a decrease in T_o/T_g , one can conclude that the Ca-based BMGs show conversion from non-Arrhenius (fragile) behavior of supercooled liquid to near-Arrhenius behavior of glass in the temperature region of the glass transition.

A similar transition from a steep temperature dependence of viscosity/relaxation time of supercooled liquid to the weaker dependence of respective glass has been earlier reported for several fragile organic liquids [29,30] as well as for metallic glasses [19,31,32]. For example, Figure 4 illustrates the temperature dependence of the viscosity of α -naphthal benzene (TaNB) [29]. The supercooled liquid of this organic glass former shows highly non-Arrhenius (fragile) behavior of the viscosity, with the fragility index $m_k = 76$ and the relaxation activation enthalpy $\Delta H_g \approx 485$ kJ/mol. At the same time, viscosity of the glass measured below T_g shows much weaker, near Arrhenius, temperature dependence with $m_k = 28$ and the relaxation activation enthalpy $\Delta H_g \approx 179$ kJ/mol. Two other examples of the weaker temperature dependence of viscosity of the glass than the respective supercooled liquid have been reported for $Zr_{46.8}Ti_{8.2}Cu_{7.5}Ni_{10}Be_{27.5}$ (Figure 3 in ref. 19) and $Mg_{65}Cu_{25}Y_{10}$ (Figure 8 in ref. 31) amorphous metallic alloys. In both cases a rapid, non-Arrhenius, increase in the liquid viscosity with a decrease in the temperature, which can be described by the VFT Equation (1), was observed. At the same time, the viscosity of a non-equilibrium glassy state was reported to show a much weaker temperature dependence, so that the difference between the equilibrium and non-equilibrium viscosities increased with a decrease in the temperature. From the slopes of $\log \eta$ vs. $1/T$ dependences near T_g [19,31], we estimated the fragility indexes m_k for the supercooled liquid and glassy states (i.e. for equilibrium and non-equilibrium amorphous states) to be, respectively, 46.0 and 17.0 for the Zr-based alloy and 50.0 and 30.5 for the Mg-based alloy. The less viscous behavior and a weaker temperature dependence of the viscosity of the non-equilibrium glass relative to the equilibrium liquid at $T < T_g$ were attributed to frozen-in excess free volume in the glass [19,33].

Because of the non-equilibrium nature of glass, its properties depend on the glass history. In particular, no well-defined equilibrium viscosity or relaxation time can be assigned to the frozen glassy state [19]. The non-equilibrium properties measured at a given temperature will continuously change with an increase in the laboratory time scale and the properties may achieve their equilibrium values (which always correspond to the properties of the supercooled liquid) only when the observation time exceeds the relaxation time. In other words, during DSC experiments with continuous heating, the onset of the glass transition always corresponds to a non-equilibrium glassy state and only the end of the glass transition corresponds to the equilibrium supercooled liquid state. An increase in the heating rate decreases the observation time at every given temperature and, therefore, shifts the glass transition toward higher temperatures where the equilibrium (supercooled liquid state) can be achieved within the time governed by the heating rate. One can therefore conclude that the rate dependence of the end of the glass transition, T_{ge} , must be used in these DSC experiments for correct computation of properties of the supercooled liquid (e.g. m_c and ΔH_g). The onset of the glass transition cannot be used for this purpose, because m_{cs} and ΔH_{gs} values determined at T_{gs} correspond to a non-equilibrium condition of the glass and, therefore, their values would depend on the glass history. This explains why the m_{cs} values obtained in DSC heating experiments and related to the onset of the glass transition are almost always smaller than the m_k values obtained from direct measurements of equilibrium viscosity / relaxation time of supercooled liquids [10,15,17]. Another important observation of this work is that the fragility indexes calculated using Equation (6) are about 10-20% smaller than those obtained with the use of Equation (7). This observation indicates that the temperature dependences of the DSC heating rate and the glass transition relaxation time are different, which is evidently due to the rate dependence of the glass transition

width ΔT_g . Indeed, as it was first discussed in [1], $\tau_g^{cal} = \Delta T_g / \varphi$ or $\frac{d \log \tau_g^{cal}}{d \log \varphi} = \frac{d \log \Delta T_g}{d \log \varphi} - 1$.

Therefore, Equations (6) and (7) for calculation of m_c will be equivalent (i.e. $d \log \tau_g^{cal} \approx -d \log \varphi$) only if the contribution from the ΔT_g containing term to m_c is less than or compared to the experimental error (generally <5%). Otherwise, Equation (6) should not be used as it would provide incorrect m_c values.

Figure 5 compares fragile behavior of the relaxation time of the equilibrium Ca-based glass-forming liquids with the behavior of vitreous GeO₂ [34], Zr_{46.75}Ti_{8.25}Cu_{7.5}Ni₁₀Be_{27.5} (Vit4) [19,35] and Mg₆₅Cu₂₅Y₁₀ [31]. The temperature dependences of the relaxation time for these three amorphous materials were deduced from the experimentally available viscosity database using Maxwell relation $\eta = G_\infty \tau$, where the dynamic modulus G_∞ is 18.1 GPa for GeO₂ [36], 37.2 GPa for Vit4 [10] and ~20 GPa for Mg₆₅Cu₂₅Y₁₀ [10]. GeO₂ is an excellent glass forming liquid, which has a critical cooling rate for amorphization $R_c \approx 0.01$ K/s [4]. It has a near Arrhenius relaxation behavior in a wide temperature range, resulting in a low fragility index $m_k = 21.8$. The Vit4 and Mg₆₅Cu₂₅Y₁₀ are two of the best bulk metallic glass formers with $R_c \approx 8$ K/s and 50 K/s, respectively [35], and exhibit relatively strong liquid behavior ($m_k = 46$ and 50 [4]). The high viscosity/relaxation time of these bulk metallic glass formers is an important contributing factor to their superior glass forming ability since it implies sluggish kinetics in the entire range of the supercooled liquid. Figure 5 illustrates that the supercooled Ca-based liquids are noticeably stronger than the Zr- and Mg-based glass-forming liquids. Extrapolation of the VFT fit to higher temperatures predicts that the relaxation time (and viscosity) of these Ca-based BMGs is about 2-2.5 orders of magnitude higher than those of Vit4 and Mg₆₅Cu₂₅Y₁₀ in the vicinity of the

equilibrium melting (i.e. at $T_g/T = 0.55 - 0.7$). This explains excellent glass forming ability of the Ca-based alloys.

Using a recently proposed relationship between R_c , $T_{rg} = T_g/T_m$ and m (Equation 3) [4], the critical cooling rate for amorphization was estimated for the Ca-based BMGs. The results are given in Table 4. The R_c values for some other BMGs, which were estimated independently by two methods: (i) from experimental temperature-time-transformation (TTT) diagrams and (ii) using Equation (3), are also presented in this table for comparison. A rather good agreement between the R_c values estimated by these two methods can be seen, indicating that Equation (3) estimates the critical cooling rates for amorphization rather well (see also [4]). Therefore, the low R_c values (~0.2 to 10 K/s) predicted by this equation for the Ca-based glasses should also be considered reliable. One can therefore conclude that the GFA of the Ca-based BMGs is similar to that of Pd- and Zr- based BMGs.

Excellent GFA of Ca-based BMGs indicates sluggish crystallization during solidification, as crystallization and glass formation are always competing processes; thus glass is formed only when crystallization is suppressed during solidification. Crystallization is thermodynamically and kinetically driven and it accompanies with the atomic rearrangements from the disordered state of liquid to a long-range ordered state of crystal. Recent thermodynamic analysis of the Ca-Mg-Zn alloy system by Gorsse et al. [3] showed that the GFA of these alloys generally improves with a decrease in the onset driving force for crystallization. Slow kinetics of crystallization due to high viscosity / high relaxation time of supercooled liquid can also be important for enhancing GFA of bulk metallic glasses [3,4]. As stronger liquids generally have higher viscosity / relaxation time between the melting and glass transition temperatures than more fragile liquids,

the crystallization kinetics of the former (at the same driving force) are generally much slower, leading to enhanced GFA.

CONCLUSIONS

Relaxation behavior of two Ca-Mg-Zn, two Ca-Mg-Cu and one Ca-Mg-Zn-Cu bulk metallic glasses was studied in the glass transition range using DSC with heating rates from 1 to 160 K/min. The temperatures of the start T_{gs} and the end T_{ge} of the glass transition increase while the glass transition temperature width $\Delta T_g = T_{ge} - T_{gs}$ decreases with an increase in the heating rate. Such behavior allows analysis and comparison of the temperature dependence of the relaxation time in the non-equilibrium glassy state near the onset of the glass transition, and in the equilibrium supercooled liquid state near the end of the glass transition. The temperature dependences of the relaxation time at the onset and at the end of the glass transition are different. The activation enthalpy of structural relaxation ΔH_g and the fragility index m are smaller in the glassy state than in the supercooled liquid state. The smaller ΔH_g indicates easier activation of the structural relaxation in the glassy state than in the supercooled liquid state at temperatures near and below T_g , which explains the reduced values of the relaxation time and viscosity of glass relative to the supercooled liquid in this temperature range. It was concluded that the heating rate dependence of the end of the glass transition should be used to correctly analyze the relaxation behavior of the supercooled liquid. The onset glass transition temperature cannot be used to analyze the equilibrium behavior because in this condition almost 100% of the material is in a non-equilibrium glassy state. The Ca-based glass-forming liquids show strong behavior of the relaxation time, with the fragility indexes m_c in the range of 33 to 40. The strong liquid behavior implies sluggish kinetics

of crystallization in the supercooled liquid region and can explain the very good glass forming ability of these alloys. The critical cooling rate for amorphization R_c of the Ca-based bulk metallic glasses was estimated to be in the range of 0.3 to 10 K/s, which is similar to R_c values for the best Pd and Zr based metallic glass forming alloys discovered so far.

ACKNOWLEDGEMENTS

Technical support from J.M. Scott (sample preparation) and S.V. Senkova (DSC experiments) is very much appreciated. This work was financially supported through the Air Force Office of Scientific Research (Dr. J. Fuller, Program Manager) and the Air Force Research Laboratory on-site contract FA8650-04-D-5235 (UES, Inc.).

FIGURE CAPTIONS

Figure 1. A DSC scan at $\varphi = 20$ K/min of the $\text{Ca}_{50}\text{Mg}_{20}\text{Cu}_{30}$ bulk metallic glass. The temperatures of the onset, T_{gs} , and the end, T_{ge} , of the glass transition, as well as the temperature of the onset of crystallization, T_x are indicated in the figure. The endothermic reactions are directed up.

Figure 2. The heating rate dependence of the temperatures of the onset (\circ) and the end (\bullet) of the glass transition for (a) $\text{Ca}_{60}\text{Mg}_{20}\text{Cu}_{20}$ and (b) $\text{Ca}_{60}\text{Mg}_{20}\text{Zn}_{20}$ BMGs.

Figure 3. The temperature dependence of the relaxation time at the onset (a) and the end (b) of the glass transition for five Ca-based BMGs. The symbols represent experimental data and dashed lines are the fits of Equation (1) with fitting parameters given in Tables 2 and 3.

Figure 4. Dependence of the logarithm of viscosity on the reciprocal absolute temperature for α -naphthal benzene (TaNB) [29]. A rapid non-Arrhenius decrease in the liquid viscosity and a much weaker, almost Arrhenius, decrease in the viscosity of the glass with an increase in the temperature are clearly seen.

Figure 5. Fragility plot of the relaxation time of five Ca-based metallic glasses from this work, $\text{Zr}_{46.75}\text{Ti}_{8.25}\text{Cu}_{7.5}\text{Ni}_{10}\text{Be}_{27.5}$ (Vit4) [19,35], $\text{Mg}_{65}\text{Cu}_{25}\text{Y}_{10}$ [31], and GeO_2 [34]. The relaxation time data for Zr-based and Mg-based BMGs were deduced from the viscosity database using the Maxwell equation, $\tau = \eta/G_\infty$, where the dynamic shear modulus G_∞ is 37.2 GPa for Vit4 and 20 GPa for $\text{Mg}_{65}\text{Cu}_{25}\text{Y}_{10}$ [10] and 18.1 GPa for GeO_2 [36].

TABLES

Table 1. The calculated activation enthalpy of structural relaxation ΔH_g (Equation 5) and fragility index m_c (Equation 6) at the onset (ΔH_{gs} , m_{cs}) and at the end ((ΔH_{ge} , m_{ce}) of the glass transition for five Ca-based bulk metallic glasses.

Glass ID	ΔH_{gs} kJ/mol	ΔH_{ge} kJ/mol	m_{cs} Eq. 6	m_{ce} Eq. 6
Ca ₆₅ Mg ₁₅ Zn ₂₀	127	211	19.4	30.5
Ca ₆₀ Mg ₂₀ Zn ₂₀	121	215	18.1	29.2
Ca ₆₀ Mg ₂₀ Cu ₂₀	125	224	18.5	29.8
Ca ₅₀ Mg ₂₀ Cu ₃₀	125	229	18.0	29.7
Ca ₅₅ Mg ₁₈ Zn ₁₁ Cu ₁₆	134	255	19.5	34.2

Table 2. Fitting parameters of the VFT Equation (1) for the onset of the glass transition of five Ca-based bulk metallic glasses. The coefficient of determination of the fit, r^2 , and the calculated T_{gs}^{ref} (the onset temperature at which $\tau_g^{cal} = 10^3$ s) and m_{cs} (Equation 7) values are also given here. The subscript 's' indicates that the parameters are associated with the onset (start) of the glass transition.

Glass ID	τ_∞ s	A_s K	T_{os} K	r_s^2	T_{gs}^{ref} K	m_{cs} Eq. 7
Ca ₆₅ Mg ₁₅ Zn ₂₀	10 ⁻¹⁴	9138	108.3	0.99866	341.7	24.9
Ca ₆₀ Mg ₂₀ Zn ₂₀	10 ⁻¹⁴	11306	61.3	0.99977	350.1	20.6
Ca ₆₀ Mg ₂₀ Cu ₂₀	10 ⁻¹⁴	11503	59.1	0.99963	353.0	20.4
Ca ₅₀ Mg ₂₀ Cu ₃₀	10 ⁻¹⁴	12231	50.8	0.99731	363.3	19.8
Ca ₅₅ Mg ₁₈ Zn ₁₁ Cu ₁₆	10 ⁻¹⁴	10726	85.8	0.99921	359.8	22.3

Table 3. Fitting parameters of the VFT Equation (1) for the end of the glass transition of five Ca-based bulk metallic glasses. The coefficient of determination of the fit, r^2 , and the calculated T_{ge}^{ref} (the temperature of the end of the glass transition at which $\tau_g^{cal} = 10^3$ s) and m_{ce} (Equation 7) values are also given here. The subscript 'e' indicates that the parameters are associated with the end of the glass transition.

Glass ID	τ_∞ S	$\log \tau_\infty$ log(s)	A_e K	T_{oe} K	r_e^2	T_{ge}^{ref} K	m_{ce} Eq. 7
Ca ₆₅ Mg ₁₅ Zn ₂₀	10^{-14}	-14	5985	206.8	0.99847	359.7	40.0
Ca ₆₀ Mg ₂₀ Zn ₂₀	10^{-14}	-14	7582	190.4	0.99481	384.1	33.7
Ca ₆₀ Mg ₂₀ Cu ₂₀	10^{-14}	-14	7693	196.5	0.9985	393.0	34.0
Ca ₅₀ Mg ₂₀ Cu ₃₀	10^{-14}	-14	8050	197.1	0.98727	402.8	33.3
Ca ₅₅ Mg ₁₈ Zn ₁₁ Cu ₁₆	10^{-14}	-14	6688	218.5	0.99749	389.4	38.7

Table 4. Reduced glass transition temperature, T_{rg} , fragility indexes, m_k and m_c , and the critical cooling rate, R_c (from TTT diagrams and given by Equation 3), for Ca-based (this work), $\text{Zr}_{46.75}\text{Ti}_{8.25}\text{Cu}_{7.5}\text{Ni}_{10}\text{Be}_{27.5}$ (Vit 4) [19,35], $\text{Zr}_{41.2}\text{Ti}_{13.8}\text{Cu}_{12.5}\text{Ni}_{10}\text{Be}_{22.5}$ (Vit1) [35], $\text{Mg}_{65}\text{Cu}_{25}\text{Y}_{10}$ [31] and $\text{Pd}_{40}\text{Ni}_{10}\text{Cu}_{30}\text{P}_{20}$ [37,38] BMGs.

Glass ID	T_{rg} (K)	m_k	m_c	R_c (K/s) TTT	R_c (K/s) Eq. (4)
$\text{Ca}_{65}\text{Mg}_{15}\text{Zn}_{20}$	0.573		40.0		4.0
$\text{Ca}_{60}\text{Mg}_{20}\text{Zn}_{20}$	0.582		33.7		0.3
$\text{Ca}_{60}\text{Mg}_{20}\text{Cu}_{20}$	0.580		34.0		0.3
$\text{Ca}_{50}\text{Mg}_{20}\text{Cu}_{30}$	0.584		33.3		0.2
$\text{Ca}_{55}\text{Mg}_{18}\text{Zn}_{11}\text{Cu}_{16}$	0.612		38.7		0.3
$\text{Zr}_{41.2}\text{Ti}_{13.8}\text{Cu}_{12.5}\text{Ni}_{10}\text{Be}_{22.5}$	0.629	46.0		1.2	1.1
$\text{Zr}_{46.75}\text{Ti}_{8.25}\text{Cu}_{7.5}\text{Ni}_{10}\text{Be}_{27.5}$	0.578	46.0		<10	15.9
$\text{Mg}_{65}\text{Cu}_{25}\text{Y}_{10}$	0.535	50.0		50	140
$\text{Pd}_{40}\text{Ni}_{10}\text{Cu}_{30}\text{P}_{20}$	0.707	59.0		0.1-0.3	0.2

FIGURES

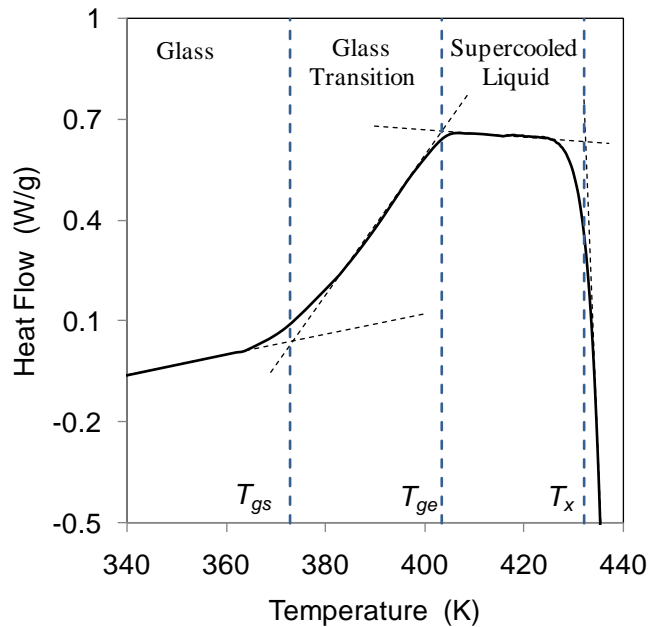
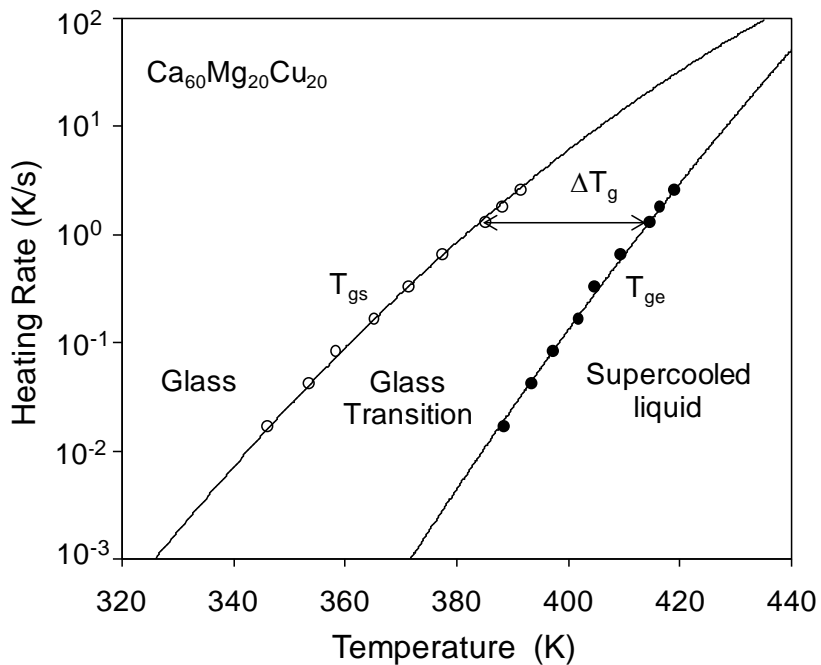
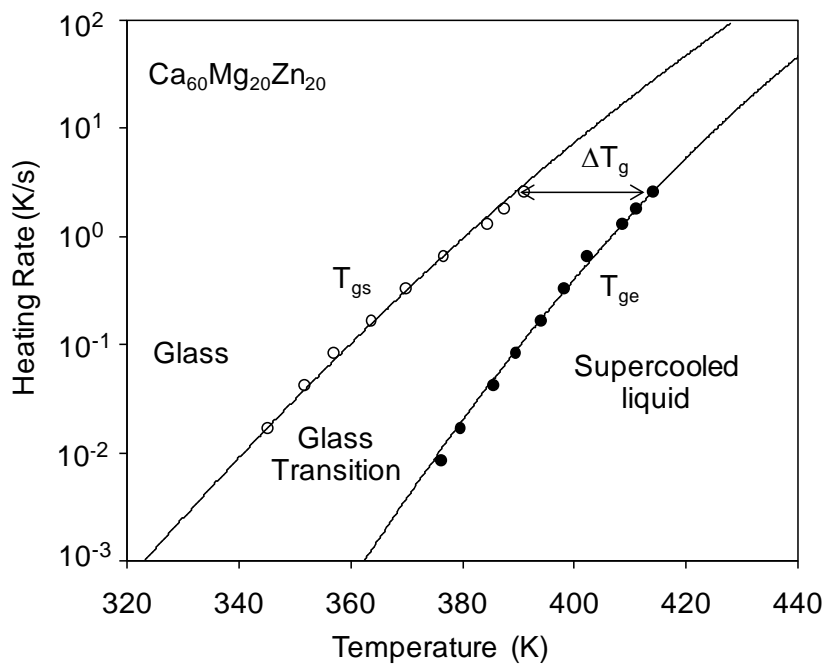


Figure 1. A DSC scan at $\varphi = 20$ K/min of the $\text{Ca}_{50}\text{Mg}_{20}\text{Cu}_{30}$ bulk metallic glass. The temperatures of the onset, T_{gs} , and the end, T_{ge} , of the glass transition, as well as the temperature of the onset of crystallization, T_x are indicated in the figure. The endothermic reactions are directed up.

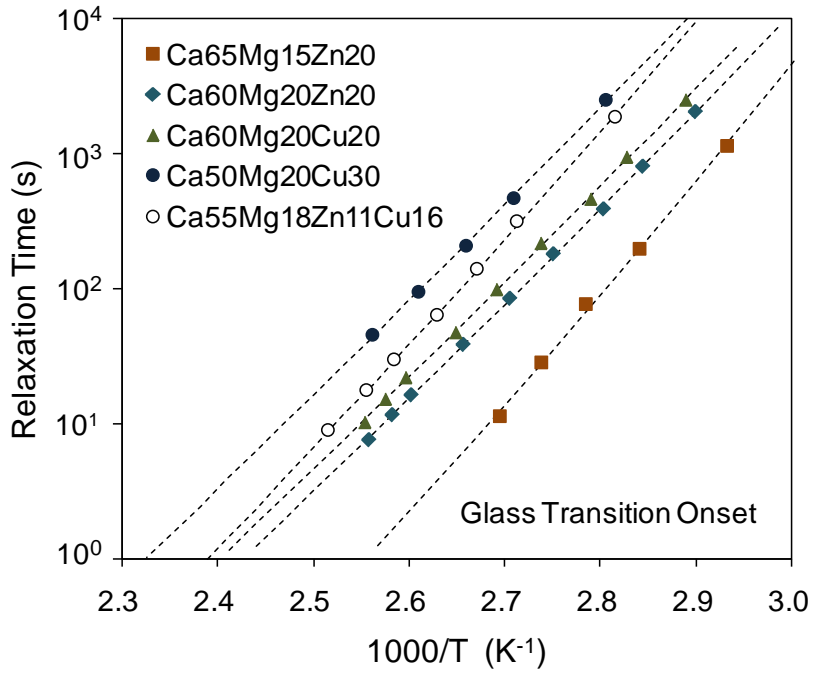


(a)

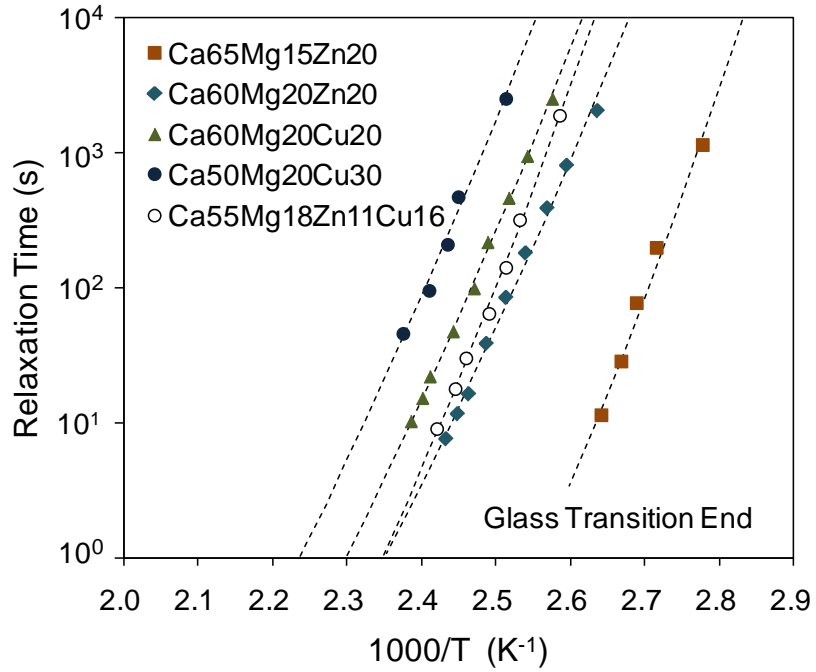


(b)

Figure 2. The heating rate dependence of the temperatures of the onset (\circ) and the end (\bullet) of the glass transition for (a) $\text{Ca}_{60}\text{Mg}_{20}\text{Cu}_{20}$ and (b) $\text{Ca}_{60}\text{Mg}_{20}\text{Zn}_{20}$ BMGs.



(a)



(b)

Figure 3. The temperature dependence of the relaxation time at the onset (a) and the end (b) of the glass transition for five Ca-based BMGs. The symbols represent experimental data and dashed lines are the fits of Equation (1) with fitting parameters given in Tables 2 and 3.

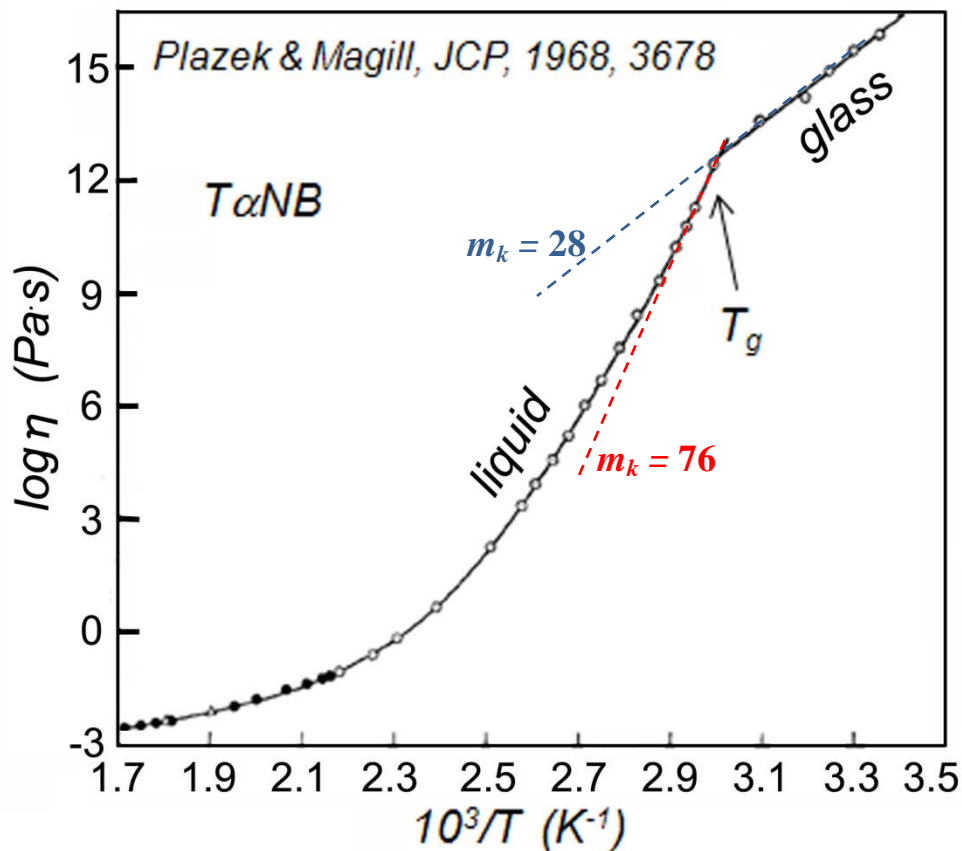


Figure 4. Dependence of the logarithm of viscosity on the reciprocal absolute temperature for α -naphthyl benzene ($T\alpha NB$) [29]. A rapid non-Arrhenius decrease in the liquid viscosity and a much weaker, almost Arrhenius, decrease in the viscosity of the glass with an increase in the temperature are clearly seen.

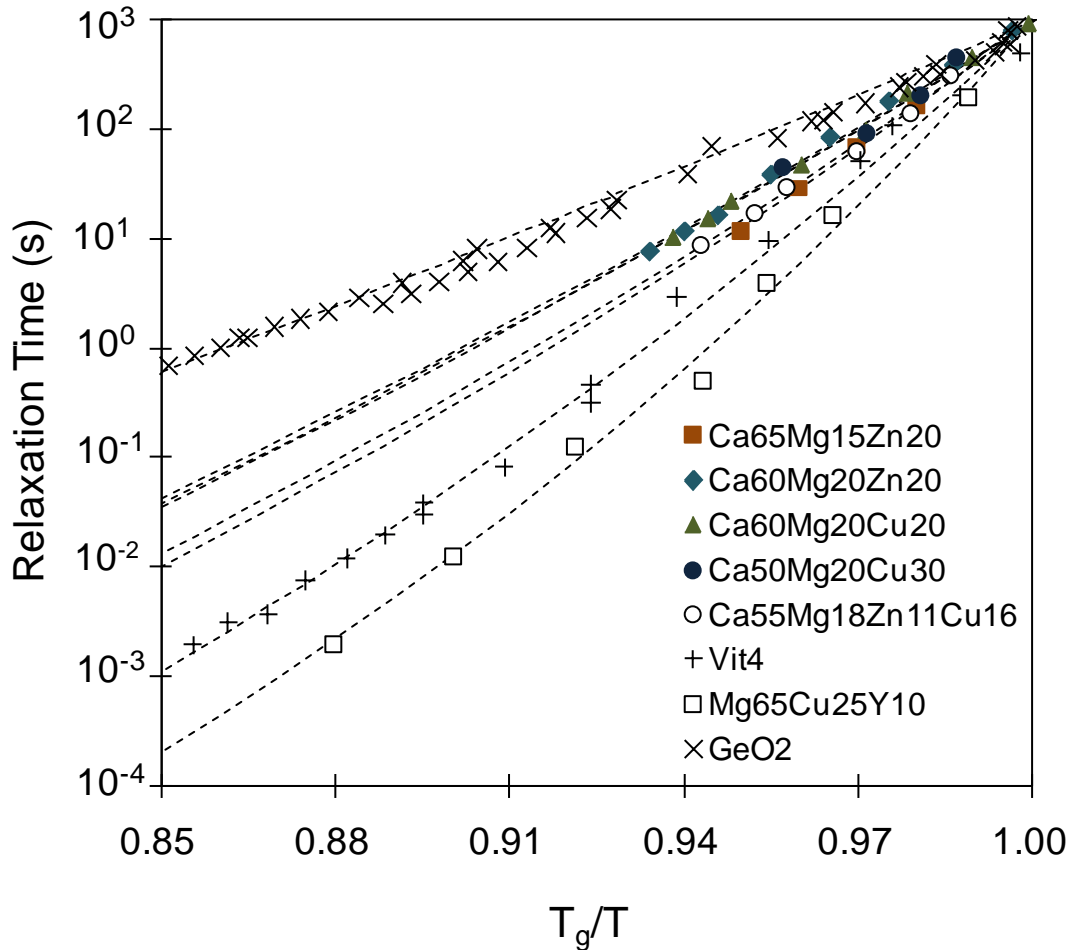


Figure 5. Fragility plot of the relaxation time of five Ca-based metallic glasses from this work, Zr_{46.75}Ti_{8.25}Cu_{7.5}Ni₁₀Be_{27.5} (Vit4) [19,35], Mg₆₅Cu₂₅Y₁₀ [31], and GeO₂ [34]. The relaxation time data for Zr-based and Mg-based BMGs were deduced from the viscosity database using the Maxwell equation, $\tau = \eta/G_\infty$, where the dynamic shear modulus G_∞ is 37.2 GPa for Vit4 and 20 GPa for Mg₆₅Cu₂₅Y₁₀ [10] and 18.1 GPa for GeO₂ [36].

REFERENCES

1. R. Brüning and T. Crowell, *J. Non-Cryst. Solids*, 1999, vol. 248, pp. 183-193.
2. M.L.F. Nascimento, E.B. Ferreira, E.D. Zanotto, *J. Chem Phys.*, 2004, vol. 121, pp. 8924-8928.
3. S. Gorsse, G. Orveillon, O.N. Senkov, and D.B. Miracle, *Phys. Rev. B*, 2006, vol. 73, pp. 224202/1-9.
4. O.N. Senkov, *Phys. Rev. B*, 2007, vol. 76, pp. 104202/1-6.
5. R. Busch, J. Schroers, and W.H. Wang, *MRS Bulletin*, 2007, vol. 32, pp. 620-623.
6. C.A. Angell, Strong and Fragile Liquids, in: K.L. Ngai and G.P. Wright (Eds.), Relaxations in Complex Systems, U.S. GPO, Washington, D.C., 1985, pp. 3-11; *J. Non-Cryst. Solids*, 1988, vol. 102, pp. 205-221.
7. R. Böhmer, K.L. Ngai, C.A. Angell, and D.J. Plazek, *J. Chem. Phys.*, 1993, vol. 99, pp. 4201-4209.
8. T. Scopigno, G. Ruocco, R. Sette, and G. Monaco, *Science*, 2003, vol. 302, pp. 849-852.
9. V.N. Novikov and A.P. Sokolov, *Nature*, 2004, vol. 431, pp. 961-963.
10. W.H. Wang, *J. Appl. Phys.*, 2006, vol. 99, pp. 093506/1-10.
11. L.M. Wang, C.A. Angell and R. Richert, *J. Chem. Phys.* 2006, vol. 125, pp. 074505/1-8.
12. O.N. Senkov and D.B. Miracle, *J. Chem. Phys.*, 2008, vol. 128, pp. 124508/1-3.
13. G.J. Fan, J.F. Loffler, R.K. Wunderlich, H.J. Fecht, *Acta Mater.*, 2004, vol. 52, pp. 667-674.
14. O.N. Senkov and D.B. Miracle, *J. Non-Cryst. Solids*, 2009 (submitted).
15. C.A. Angell, *J. Res. NIST*, 1997, vol. 102, pp. 171-185.
16. D.N. Perera, *J. Phys.: Condens. Matter*, 1999, vol. 11, pp. 3807-3812.

-
17. C.T. Moynihan, A.J. Easteal, J. Wilder, and J. Tucker, *J. Phys. Chem.*, 1974, vol. 78, pp. 2673-2677.
 18. R. Brüning and K. Samwer, *Phys. Rev. B*, 1992, vol. 46, pp. 11318-11322.
 19. R. Busch, E. Bakke, and W.L. Johnson, *Acta Mater.*, 1998, vol. 46, pp. 4725-4732.
 20. B.A. Legg, J. Schroers, and R. Busch, *Acta Mater.*, 2007, vol. 55, pp. 1109-1116.
 21. O.N. Senkov and J.M. Scott, *J. Non-Cryst. Solids*, 2005, Vol. 351, pp. 3087-3094.
 22. O.N. Senkov and D.B. Miracle, in: T.S. Srivatsan, R.A. Varin, R. Abbaschian, S. Viswanathan, (Eds.), *Processing and Fabrication of Advanced Materials XIV*, ASM International, Pittsburgh, PA, 2005, pp. 249-266.
 23. O.N. Senkov, D.B. Miracle, and J.M. Scott, *Intermetallics*, 2006, Vol. 14, pp. 1055-160.
 24. O.N. Senkov, J.M. Scott, and D.B. Miracle, *J. Alloys Compounds*, 2006, Vol. 424, pp. 394-399.
 25. O.N. Senkov, D.B. Miracle, V. Keppens, and P.K. Liaw, *Mater. Trans. A*, 2008, vol. 39A, pp. 1888-1900.
 26. E.S. Park and D.H. Kim, *J. Mater. Research*, 2004, vol. 19, pp. 685-688.
 27. E.S. Park, W.T. Kim and D.H. Kim, *Mater. Sci. Forum*, 2005, vol. 475-479, pp. 3415-3418.
 28. O.N. Senkov and J.M. Scott, *Scripta Mater.*, 2004, vol. 50, pp. 449-452.
 29. D.J. Plazek and J.H. Magill, *J. Chem. Phys.* 1968, vol. 49, pp. 3678-3682
 30. W.T. Laughlin and D.R. Uhlmann, *J. Phys. Chem.*, 1972, v. 76, pp. 2317-2325.
 31. R. Busch, W. Liu, and W.L. Johnson, *J. Appl. Phys.*, 1998, vol. 83, pp. 4134-4141.
 32. O.P. Bobrov, V.A. Khonik, S.A. Lyakhov, K. Cgach, K. Kitagawa, and H. Neuhauser, *J. Appl. Phys.*, 2006, vol. 100, pp. 033518/1-9.
 33. R. Busch and W.L. Johnson, *Appl. Phys Lett.*, 1998, vol. 72, pp. 2695-2697.

-
- 34. A. Sipp, Y. Bottinga, P. Richet, *J. Non-Cryst. Solids*, 2001, vol. 288, pp. 166-174.
 - 35. S.C. Glade and W.L. Johnson, *J. Appl. Phys.*, 2000, vol. 87, pp. 7249-7251.
 - 36. L.G. Hwa, W.C. Chao, S.P. Szu, *J. Mater. Sci.*, 2002, vol. 37, pp. 3423-3427.
 - 37. A. Takeuchi and A. Inoue, *Mater. Sci. Eng. A*, 2004, vol. 375-377, pp. 449-454.
 - 38. J.F. Löffler, J. Schroers, and W.L. Johnson, *Appl. Phys. Lett.*, 2000, vol. 77, pp. 681-683.